water

MDPI

Article

Multivariate Statistical Analysis of the Spatial Variability of Hydrochemical Evolution during Riverbank Infiltration

Yingjie Bo [1,2,3], Yaoxuan Chen [2,3,4,*], Qiaohui Che [1,2,3], Yakun Shi [5] and Yiwu Zhang [6]

[1] College of Construction Engineering, Jilin University, Changchun 130021, China
[2] Key Laboratory of Groundwater Resources and Environment, Ministry of Education, Jilin University, Changchun 130026, China
[3] Institute of Water Resources and Environment, Jilin University, Changchun 130026, China
[4] China Institute of Geo-Environmental Monitoring, Beijing 100081, China
[5] No. 1 Institute of Geo-Environment Survey of Henan, Zhengzhou 450000, China
[6] Nanjing Center, China Geological Survey, Nanjing 210000, China
* Correspondence: chenyaoxuan_jlu@163.com

Abstract: Riverbank filtration (RBF) is increasingly being used as a relatively cheap and sustainable means to improve the quality of surface water. Due to the obvious differences in physical, chemical, and biological characteristics between river water and groundwater, there are strong and complex physical, chemical, and biogeochemical effects in the process of bank filtration. In this paper, multivariate statistical analysis was used to identify the spatial variation of hydrogeochemical groundwater in the process of bank filtration. Firstly, the evolution process of groundwater hydrochemistry during the filtration process was identified through factor analysis. According to the results, the evolution of groundwater hydrochemistry in this area is attributable to four main types of reactions: (1) Leaching; (2) Regional groundwater influence; (3) Aerobic respiration and denitrification; and (4) Mn (IV)/Fe (III)/SO_4^{2-} reduction. According to the similarity of the geochemistry, the flow path could be divided into four different hydrochemical zones through cluster analysis, revealing the evolution law of groundwater hydrochemistry and its main influencing factors during riverbank infiltration. Large hydraulic gradient in The Zone Strongly Influenced by River Water (The first group) resulted in a weak effect of leaching on groundwater chemistry. Reoxygenation and microorganism respiration occurred in The Zone Moderately Influenced by River Water (The second group), The Zone Weakly Influenced by River Water (The third group), and The Zone Strongly Influenced by Regional Groundwater (The fourth group), resulting in fluctuations in Eh and pH values of groundwater. As a result, sulfate reduction and Mn (IV) and Fe (III) reduction alternated along the flow path. The Zone Strongly Influenced by Regional Groundwater (The fourth group) groundwater chemistry was mainly affected by regional groundwater.

Keywords: multivariate statistical analysis; bank filtration; hydrogeochemical zone

Citation: Bo, Y.; Chen, Y.; Che, Q.; Shi, Y.; Zhang, Y. Multivariate Statistical Analysis of the Spatial Variability of Hydrochemical Evolution during Riverbank Infiltration. *Water* **2022**, *14*, 3800. https://doi.org/10.3390/w14233800

Academic Editor: Fernando António Leal Pacheco

Received: 17 August 2022
Accepted: 16 November 2022
Published: 22 November 2022

1. Introduction

The growth of populations near rivers and the development of industry and agriculture make rivers vulnerable to industrial wastewater, intensive agricultural pesticide runoff and urban sewage [1,2]. RBF is a technique in which water is purified by passing it through riverbanks. This technique increases the availability of water sources by stimulating groundwater recharge by rivers. At the same time, it effectively removes suspended solids, bacteria, viruses, and heavy metals through natural attenuation processes to achieve efficient improvement of water quality [3–5]. Therefore, RBF is widely used. However, RBF through groundwater pumping leads to groundwater redox zonation along the

water flow path [6,7]. Consequently, O_2, NO_3^-, Mn(IV), Fe(III), and SO_4^{2-} are reduced successively to form redox zonation, as shown in Figure 1 [8,9]. Redox zonation during bank filtration will be at different scales and have different zonation characteristics [10].

The sequential reduction reactions during RBF can also lead to incomplete removal of organic carbon, suspended solids and inorganic contaminants, possibly leading to the presence of metals and metalloids in infiltrating river water [11]. For example, during RBF, oxides or hydroxides of iron and manganese are reduced and dissolved, and arsenic adsorbed on the surface of the medium or co-precipitated is released into groundwater [12]. This leads to the deterioration of groundwater quality and poses a serious threat to water supply security. Therefore, although RBF can remove various water pollutants, it may also damage the quality of bank filtrate and affect human and animal health. Therefore, it is important to investigate redox zonation during RBF to improve the understanding of river pollutants migration and their removal [13,14]. However, many factors affect the formation of redox zonation, such as light, temperature, pH, redox potential, oxygen, and organic carbon that affect microbial activity, river stage and groundwater level, intensity pumping, lithology, and the structure of aquifer medium and groundwater recharge conditions [15–20]. In addition, some interaction processes control the transport, fate, and reactivity of inorganic substances, including sorption, dissolution, precipitation, and mixing [11]. This may affect groundwater quality. However, it is difficult to accurately describe the complex process of water chemical evolution by analyzing the effect of single index on redox zoning.

Large datasets generated through long-term surveys and water quality monitoring projects are often difficult to analyze and explain. It is essential to extract meaningful information, such as spatio-temporal changes, important parameters, and potential pollution sources, from datasets using statistical methods without losing useful information [21,22]. Statistical analysis based on multivariate statistical theory, such as correlation matrix (CM), cluster analysis (CA), principal component analysis (PCA), factor analysis (FA), and discriminant analysis (DA), can be used to study the relationship and influence between variables. By extracting the mathematical characteristics of the data, water quality factors can be described macroscopically, and the spatiotemporal distribution of hydrochemistry can then be analyzed [23]. This improves the understanding of the geological origin and environmental origin of soluble ions and metals in water [24].

The CM can identify the relationship between parameters to understand the main factors affecting the distribution of these parameters in groundwater resources. PCA, FA, CA and are effective methods for discovering dispersed common trends and anomalies, reducing the initial dimension of the dataset, and improving the understanding of the geological and environmental sources of soluble ions and metals in water [25,26]. FA and CA have been widely used to identify chemical processes that affect water chemistry to delineate different chemical regions [27]. Choi classified redox zones in vertical order using FA and CA and determined the main geochemical processes affecting each zone [28]. Rui Zuo used PCA to analyze the similarities and differences of redox index in horizontal and vertical directions and divide redox zone [29]. However, previous studies were limited to local areas near the riverbank, and the whole flow path of river water infiltration was not analyzed.

The Kaladian riverside well field in Songyuan City, Northeast China, provides drinking water to residents. However, eutrophication and nitrogen pollution in river water are becoming more and more serious, and groundwater in the riverside well field is also facing potential risk of nitrogen pollution. The aquifer medium of the riverside well field is rich in primary minerals of high iron and manganese, and the content of iron and manganese in groundwater generally exceeds the standard. This area has primary low-quality groundwater characterized by high contents of iron and manganese ions. By analyzing the spatial distribution characteristics of groundwater environment indices and chemical components, previous studies have classified groundwater redox zones in water flow paths during bank filtration using traditional methods [16,30–32]. However, previous

studies did not comprehensively consider the influence of DOC concentration, pH value and other factors on sensitive elements in water flow paths during bank filtration. The effects of leaching and mixing on hydrochemistry were also less considered. In this study, taking the riverside well field in Songyuan, northeast China as the study area, MSA was used to further analyze the hydrochemical data, evaluate the hydrogeochemical effect, and determine key factors controlling groundwater quality in the process of river water infiltration. The results are expected to help managers to establish a better groundwater management model and understand the causes of iron and manganese pollution in groundwater by dividing hydrogeochemical zones to control groundwater pollution.

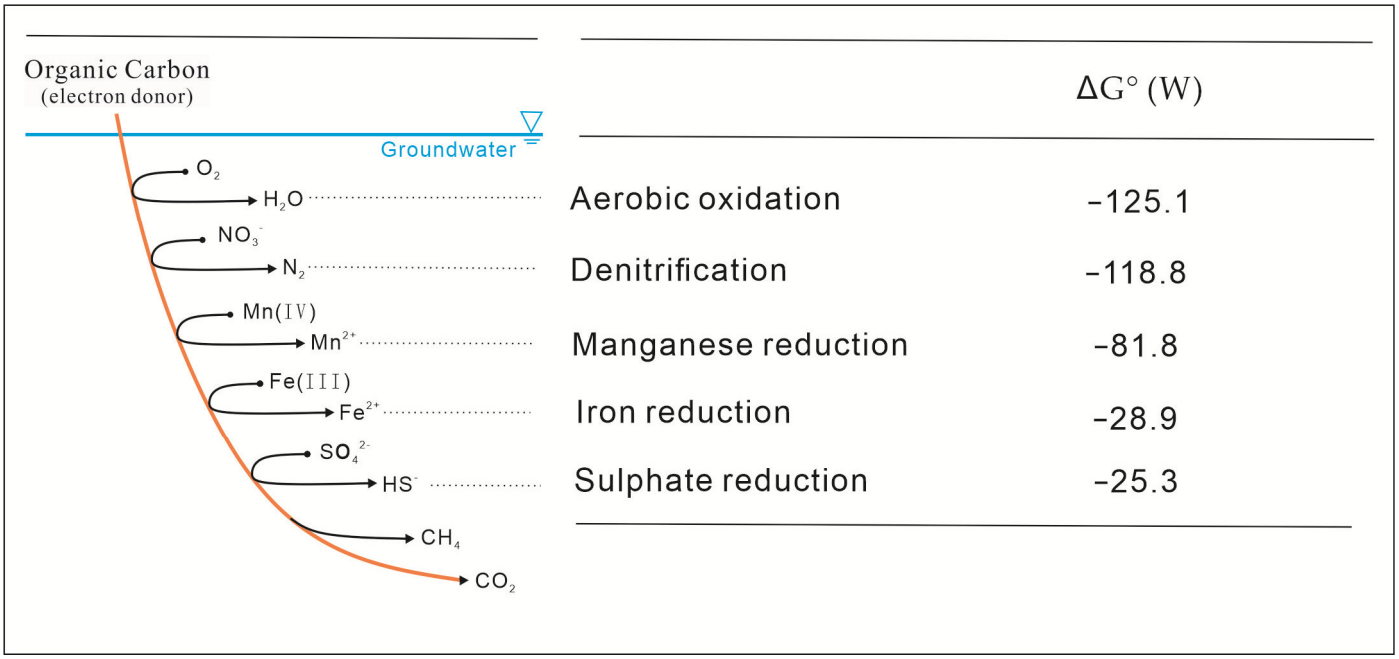

Figure 1. Electron acceptor thermodynamic sequence of organic carbon oxidation in saturated regions [8,16,31].

2. Materials and Methods

2.1. Site Description

The study area is located in northeast China. It has a flat terrain with elevation between 131 m and 136 m. The annual average temperature in the study area is 4.7 °C, the annual average rainfall is 425.7 mm, and the annual evaporation is 1594 mm. As the largest river system in Jilin Province, the Second Songhua River flows through the north of the study area from southeast to northwest. The water depth and width of the river surface are 400–450 m and 3–7 m, respectively. The annual average runoff is 476.0 m^3/s. During the dry season, which generally occurs in May, the minimum runoff is 63.3 m^3/s, and the water level is 130.12 m. During the wet season, which usually occurs in August, the maximum runoff is 6750 m^3/s and the water level is 134.96 m. The annual water level varies from 1.8 m to 4 m, with strong seasonal variations. It is higher during July–September and lower during October–March. The content of fine particles in the nearshore riverbed (within 100 m from shore) is high, and the vertical permeability is poor. The Kv value is 4.82~6.57 m/d, with an average of 5.82 m/d. In the far-bank riverbed (100~400 m from shore), the content of coarse particles in the surface sediments is high, the vertical permeability is better, and the Kv value is large, 36.39~59.37 m/d, with an average of 48.93 m/d.

The groundwater is mainly hosted in the 17–20 m phreatic aquifer. The aquifer has a loose sand and gravel structure, with good sorting and roundness. The upper and lower parts are composed of fine sand and medium sand, respectively, with a thin layer of silty

clay in the middle. The phreatic aquifer has good permeability, and its permeability coefficient is 28.14~72.79 m/d, with an average of 48.01 m/d. The floor of the aquifer is a continuous and stable clay layer of 24 m thickness.

Groundwater recharge is primarily facilitated by river water infiltration and regional groundwater lateral runoff, and discharge mainly occurs through artificial exploitation and lateral discharge. Due to the long-term mining in the water source, the groundwater drawdown funnel in the long axis direction is approximately parallel to the second Songhua River, and the funnel center is located near the C5-C6 pumping wells, as shown in Figure 2.

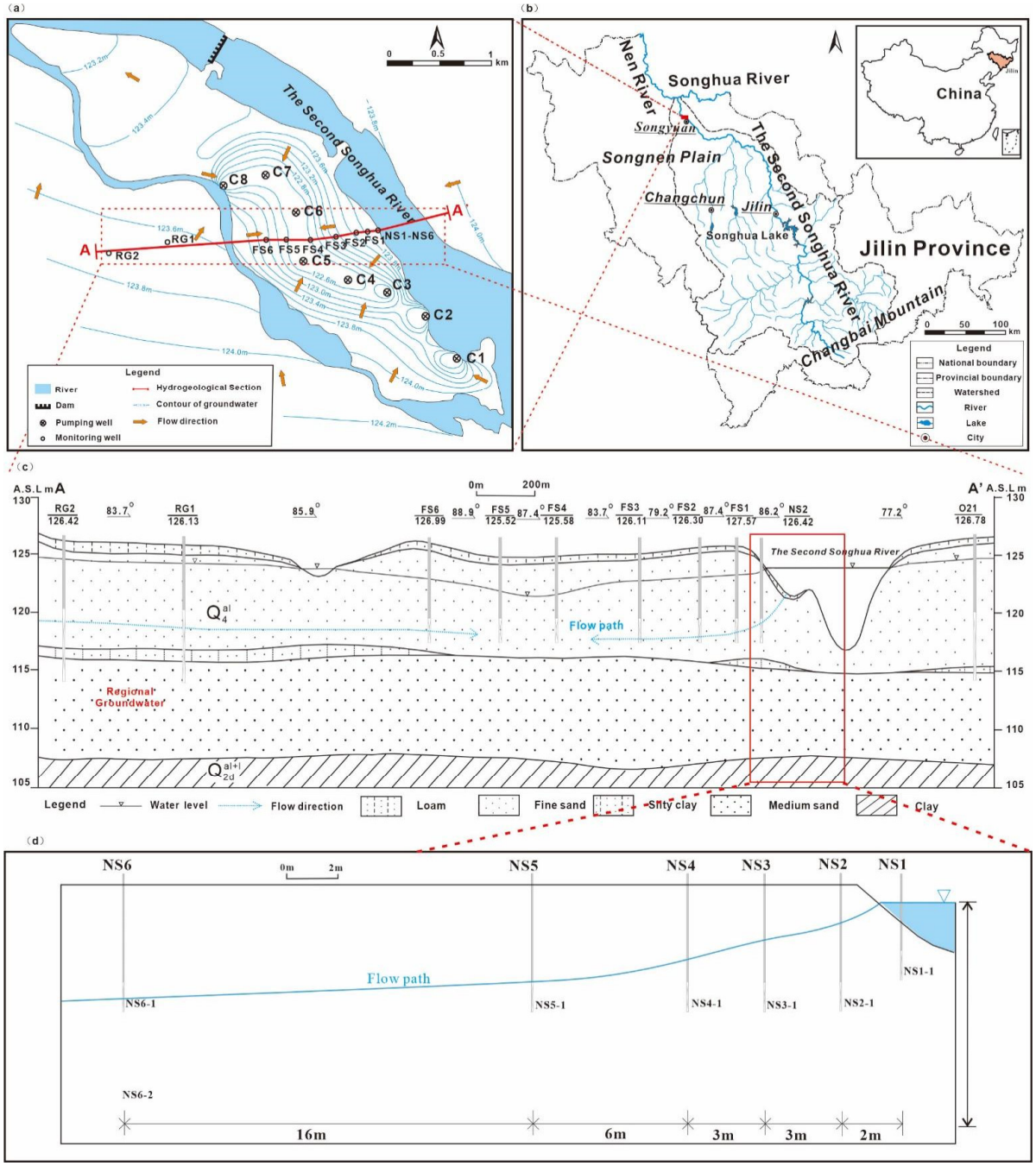

Figure 2. Distribution of wells in the study area (**a**); administrative division of the study area (**b**); flow paths and zone division by the hydrogeology condition (**c**); monitoring wells in the nearshore zone (**d**): modifications of those reported by Su et al. (2020). A-A′ represents the groundwater dynamic monitoring profile that is nearly consistent with the direction of river water infiltration into groundwater. [16].

2.2. Sampling and Analysis

The observation network of river water and groundwater established in previous studies [30]. 12 observation wells were arranged in the direction of river water infiltration to recharge groundwater (Figure 2). Monitoring point NS1 was set up in the riverbed for observations at 4 m below the riverbed. The area near the riverbank is the most obvious gradient of hydrodynamic conditions and environmental changes in the process of river water infiltration, and it is also the most active area of biogeochemistry, so the detection wells are densely arranged. Near-shore monitoring points NS1, NS2, NS3, NS4, NS5, and NS6 were set at 0 m, 2 m, 5 m, 8 m, 14 m, and 30 m away from the river, and the far-shore monitoring points FS1, FS2, FS3, FS4, FS5, and FS6 were set at 200 m, 420 m, 700 m, 850 m, and 1110 m away from the river. The well depth and filter depth of all monitoring points were 7.5 m and 6–7.5 m, respectively. Regional Groundwater detection wells RG1 and RG2 were set up in two regions at distances of 2100 m and 2700 m from the riverbank, with a depth of 12 m and a filter depth of 10.5–12 m.

In this study, river water and groundwater samples were collected in September 2018. The river water samples were collected at 20 cm below the river surface. Before collection, the sampling wells were pumped to more than three times the volume of water in the well pipe, and the sampling bottles were washed three times. Subsequently, samples were collected in the bottles at a rate of <5 L/min.

Groundwater samples for K^+, Na^+, Ca^{2+}, Mg^{2+}, Cl^-, SO_4^{2-}, HCO_3^-, NO_3^-, and NH_4^+ analyses were loaded into polyethylene bottles. Concentrated sulfuric acid was added to groundwater samples for NH_4^+ analysis in order to adjust the pH to <2. Groundwater samples for Mn^{2+} analysis were loaded into brown glass bottles and dilute hydrochloric acid was added to adjust the pH to <2. Samples for DOC were filtered with a 0.45 μm aluminum membrane and loaded into brown glass bottles, and its pH was adjusted to <2 by adding concentrated sulfuric acid. Isotope samples were filtered through a 0.22 μm filter membrane, packed into polyethylene bottles, and stored at −4 °C. δ^2H, $\delta^{18}O$ stable isotope samples using 500 mL thick-walled polyethylene bottles, sampling with sealing film sealed, stored at −4 °C environment.

T, DO, Eh, pH, total dissolved solids (TDS), and electrical conductivity (EC) were measured on-site using the Hach HQ40d portable multimeter (Hach Company, Loveland, CO, USA). Fe^{2+} and HS^- concentrations were measured on-site using Hach DR1900. The concentrations of K^+, Na^+, Ca^{2+}, Mg^{2+}, Cl^- and SO_4^{2-} in river water and groundwater were measured using an ion chromatograph (881 Compact IC pro, Metrohm, Switzerland) at the Institute of Water Resources and Environment, Jilin University (Changchun, China). The concentration of Mn^{2+} in water was tested using an atomic absorption spectromete. The mass concentrations of NO_3^- and NH_4^+ in water were tested using a continuous flow spectrometer (San++, Skalar, Netherlands) at the Institute of Water Resources and Environment, Jilin University (Changchun, China). The δ^2H and $\delta^{18}O$ values were tested using a laser isotope meter (L2140-i, Picarro, USA) at the Third Institute of Oceanography, Ministry of Natural Resources (Xiamen, China), with accuracies of ±0.50 and ±0.20‰, respectively. This paper verified hydrochemical analysis by examining ion balance.

The mass concentration of DOC in water was tested using a TOC analyzer (TOC-LCPH Shimadzu, Japan) at the Northeast Institute of Geography and Agroecology, Chinese Academy of Sciences (Changchun, China).

2.3. Multivariate Statistical Analysis(MSA)

MSA, which includes PCA, FA, CA, DA, and other commonly used methods, is conducted to determine the genesis of groundwater, speculate pollution sources, and analyze hydrogeochemical processes. In this study, FA was used to analyze the T, Eh, DO, TDS, electrical conductivity (EC), pH and main hydrochemical indexes (K^+, Na^+, Ca^{2+}, Mg^{2+}, Cl^-, SO_4^{2-}, NO_3^-, HCO_3^-, Fe^{2+}, Mn^{2+}, NH_4^+), dissolved organic carbon (DOC), and δ^2H /$\delta^{18}O$ values of river water and groundwater samples. Then, hierarchical CA (HCA) was conducted to analyze the scores of the main factors. In this paper, FA and CA was applied using IBM SPSS Statistics 25.

2.3.1. Factor Analysis (FA)

R-type FA is a type of data simplification technique. By studying the original variables with good interrelationship, the basic data structure is represented by simplified common factors, which are irrelevant or orthogonal to each other [23,33]. FA mainly involves the following steps. Firstly, the correlation matrix of the original data is calculated. Then, the eigenvalues and eigenvectors are calculated, and a set of mutually perpendicular principal component (PC) axes are designed. Finally, the new group of variables is extracted through rotating the axis defined by PCA [34–36]. The maximum variance method rotates the variables such that the loading of all variables of the factor is close to 1, 0, and −1. Loadings close to 1 reflect strong correlation with the main factor, and surface factors close to 0 indicate no significant correlation with the variables [33,37–39]. Variables with rotating loads greater than 0.5 are considered significant [36].

2.3.2. Cluster Analysis (CA)

CA is an unsupervised multivariate technique, which can be used to classify objects with similar characteristics. HCA can be used to cluster objects with similar properties through successive aggregation according to the similarity between variables or samples [40,41]. In this process, the most similar observations are first connected, and the next most similar observations are then linked. The difference between observations is represented by the Euclidean distance. The greater the Euclidean distance, the smaller the similarity between observations [37,42]. When CA is applied, the original data matrix set is normalized to dimensionless values to replace the original variables, and the Euclidean distance is then calculated. An appropriate link algorithm is used to cluster and isolate objects with larger distances [34,43–45]. In this study, the Euclidean distance and nearest domain method were used for CA. The sample position is regarded as a variable and the factor score is regarded as an object. The tree diagram provides an image summary of the clustering results, showing the grouping and proximity, and reducing the dimension of the original data. Overall, the FA and CA of groundwater samples in September 2018 were performed in SPSS. 25 to identify the hydrological and geochemical effects and their influencing factors in the process of river water infiltration.

3. Results and Discussion

3.1. Hydrodynamics of River Water and Groundwater

According to the observation data of river level from 2016 to 2018 (Figure 3), the annual variation of river level is between 1.0 and 3.2 m. The high-water level appears from July to September, and the low water level appears from October to March of the next year. In point NS1-NS6 near the coast, the groundwater level responds quickly to changes in river levels. The groundwater level along NS1–NS6 ranges from 2.8 m to 3.0 m, clearly affected by changes in river level. The water level along FS1–FS6 ranged from 0.9 m to 1.8 m, weakly affected by changes in river level. In particular, FS3–FS6 is located within the depression cone, and the water level is greatly affected by pumping instead of river levels.

In September 2018, the hydraulic gradients along the river to NS1 (within 2 m from the bank), NS1–NS6 (2–30 m from the shore), NS6–FS3 (30–420 m from the shore), and

FS3–FS4 (420–700 m from the shore) were 79.53‰, 8.62‰, 2.12‰, and 2.63‰, respectively.

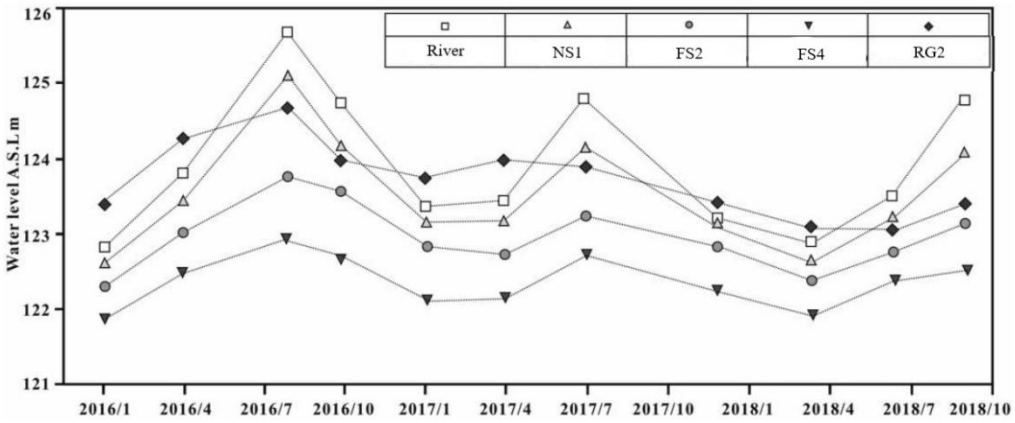

Figure 3. Water level dynamics of river and groundwater. [16].

3.2. Distribution of δ^2H and $\delta^{18}O$ in River Water and Groundwater

In this study, the ^2H and ^{18}O stable isotope data of atmospheric precipitation in Harbin station of Global Network of Isotopes in Precipitation (GNIP), which is about 150 km away from the study area, are used as Figure 4. The data are analyzed by least squares regression (LSR) to obtain LWML. The Global Meteoric Water Line (GMWL) and LMWL are shown in Figure 4.

Samples of river water and 11 wells (NS2, NS4, NS5, NS6, FS1, FS2, FS3, FS4, FS6, RG1 and RG2) were collected to test δ^2H and $\delta^{18}O$ values. River water is the main recharge source of groundwater in the study area. The Second Songhua River originates in the Changbai Mountain (altitude: 2750 m). Affected by the elevation, hydrogen and oxygen isotopes are relatively depleted in the river water, with average $\delta^{18}O$ and δ^2H values of −9.28‰ and −71.24‰, respectively. The regional groundwater is affected by evaporation, and the hydrogen and oxygen isotopes are relatively enriched, with average $\delta^{18}O$ and δ^2H values of −8.08‰ and −68.67‰, respectively.

The $\delta^{18}O$ and δ^2H values of groundwater increased gradually along the flow path, and the values along NS1–FS2 were closer to those of river water. The average values of $\delta^{18}O$ and δ^2H from NS1 to FS2 were −8.89‰ and −71.72‰, respectively. The $\delta^{18}O$ and δ^2H values along FS3–FS6 were higher than those along NS1–FS2 but significantly lower than those at FS6, with average values of −8.39‰ and −70.47‰, respectively. The $\delta^{18}O$ and δ^2H values at FS6 were close to those of the regional groundwater, with values of −6.62‰ and −60.77‰, respectively. Overall, the variation of $\delta^{18}O$ and δ^2H values along the horizontal indicates that the recharge intensity of river water to groundwater decreases gradually along the flow path, and the recharge intensity of regional groundwater increases gradually.

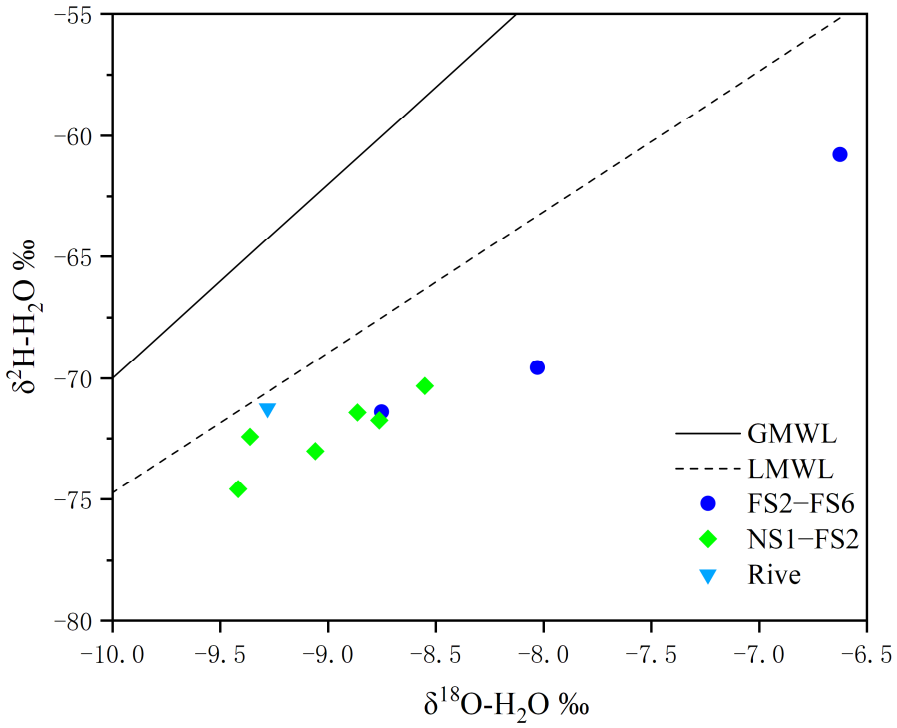

Figure 4. Distribution of $\delta^{18}O$~$\delta^{2}H$ Values in River Water and Groundwater.

3.3. Hydrochemical Indexes in River Water and Groundwater

3.3.1. Eh and DO

The Eh value of river water was 146 mV and DO content was 8.32 mg/L. The regional groundwater was found to be under a reducing environment. The average Eh and DO content of regional groundwater were −151.62 mV and 0.68 mg/L, respectively. The Eh of groundwater widely fluctuated, ranging from −48 mV to −220 mV. The average Eh from the river to FS1 was relatively low at −164.29 mg/L, and the average Eh along FS2–FS6 was relatively high at −77.93 mg/L. The fluctuation of DO was relatively small, ranging from 0.48 mg/L to 1.33 mg/L.

3.3.2. pH

The pH values of river water and regional groundwater were 7.76 and 7.11, respectively. The pH value of groundwater is affected by many factors such as recharge and discharge conditions, oxidation and reduction, and human activity, and fluctuates widely along the direction of river water infiltration. Between 420 m and 700 m from the shore, the pH value of groundwater decreased to the lowest, with an average of 7.31.

3.3.3. NO_3^- and NH_4^+

The average values of NO_3^--N and NH_4^+-N in river water were 2.28 mg/L and 0.14 mg/L, respectively. NO_3^- in regional groundwater was generally below the detection limit, and the average value of NH_4^+-N was 2.01 mg/L. The NO_3^--N concentration in groundwater decreased rapidly to the lowest value (0.02 mg/L) at NS1, and the NO_3^--N concentration along NS1–FS6 fluctuated slightly, with an average of 0.97 mg/L. The NH_4^+-N concentration increased significantly from the river to NS1, whereas it showed little change along NS1–FS6, with an average of 1.52 mg/L.

3.3.4. Mn^{2+} and Fe^{2+}

The contents of Mn^{2+} and Fe^{2+} were very low in river water but very high in regional groundwater. The concentrations of Mn^{2+} and Fe^{2+} in river water were lower than 0.1

mg/L, and those in regional groundwater were 6.03 mg/L and 12.46 mg/L, respectively. Mn^{2+} and Fe^{2+} in groundwater were higher along the direction of water infiltration, reaching the peak at NS6 and NS2, respectively, after which they decreased along the flow path. The concentrations of Mn^{2+} and Fe^{2+} in FS3 and FS4 increased significantly, and the concentrations of Mn^{2+} and Fe^{2+} along FS4–FS6 first decreased and then increased.

3.3.5. SO_4^{2-}

The average concentrations of SO_4^{2-} in river water and regional groundwater were 29.42 mg/L and 62.65 mg/L, respectively. The fluctuation of SO_4^{2-} content from the river to NS5 was small, with an average value of 32.90 mg/L. The content of SO_4^{2-} gradually decreased to 11.18 mg/L along NS5–FS2 and significantly increased from 11.18 mg/L to 74.95 mg/L along FS2–FS4. The content of SO_4^{2-} decreased significantly from 74.95 mg/L to 26.87 mg/L along FS4–FS5 and showed little change along FS5–FS6.

3.3.6. Cl^- and Na^++K^+

The concentrations of Cl^- and Na^++K^+ in river water were 14.04 mg/L and 17.86 mg/L, respectively, while those in regional groundwater were 142.90 mg/L and 156.16 mg/L, respectively. The concentrations of Cl^- and Na^++K^+ in groundwater gradually increased along the flow path, reaching the highest values in FS6 at 92.37 mg/L and 63.26 mg/L, respectively.

3.3.7. Ca^{2+}, Mg^{2+}, and HCO_3^-

The average values of Ca^{2+}, Mg^{2+}, and HCO_3^- within 80 m from the shore were 68.19 mg/L, 11.59 mg/L, and 10.69 mg/L, respectively, while the average values within 80–1100 m from the shore were 103.14 mg/L, 19.53 mg/L, and 27.25 mg/L, respectively. In the process of river water infiltration, the hydraulic gradient gradually decreased, the seepage velocity decreased, and the time of water passing through the sediments increased. With the weathering and hydrolysis of carbonate and silicate minerals by groundwater, Ca^{2+}, Mg^{2+}, and HCO_3^- were enriched in groundwater.

3.4. Factor Analysis

In this study, FA was performed on 20 chemical parameters, including pH, Eh, DO, EC, TDS, T, main hydrochemical indexes (K^+, Na^+, Ca^{2+}, Mg^{2+}, Cl^-, SO_4^{2-}, HS^-, NH_3^+, NO_3^-, Mn^{2+}, Fe^{2+}, HCO_3^-), and δ^2H, $\delta^{18}O$ values. The Kaiser-Meyer-Olkin (KMO) test and Bartlett's test of sphericity were performed, and the results showed that the KMO values were greater than 0.5. Regarding the KMO test, the general value of above 0.5 indicates acceptable applicability, and for the Bartlett's sphericity test, sig = 0 indicates that the hydrochemical parameters of the sample are suitable for FA. The eigenvalues of the four factors were greater than 1 and the cumulative contribution rate was 92.6%, which showed that the extracted main factor represented most of the information of the original data. According to the absolute value of factor loadings, the factor load of each variable was divided into strong (>0.75), medium (0.75–0.5), and weak (0.5–0.3) [46]. Based on these criteria, each factor was defined, and the results indicate that major factors governing the groundwater quality of this aquifer are leaching (F1), groundwater influence (F2), aerobic respiration and denitrification (F3), and Mn (IV)/Fe (III)/SO_4^{2-} Reduction (F4).

The variance contribution rate of factor 1 (F1) is 33.75% as shown in Table 1. F1 shows strong positive loading for Ca^{2+}, NH_4^+, HCO_3^-, Mg^{2+}, EC, and TDS. Strong positive loadings show high linear correlation between factors and variables. Some studies have shown that the type of bicarbonate water is mainly produced by the dissolution of calcite, dolomite, and gypsum. It was found that the content of Ca^{2+}, Mg^{2+}, HCO_3^-, SO_4^{2-} and TDS increased in the bank filtration system of Hulan River in China and Ganges River in India. It was found that the content of Ca^{2+}, Mg^{2+}, HCO_3^-, SO_4^{2-} and TDS increased due to leaching [47,48]. The score for F1 also increases along the direction of river recharge to groundwater. As water flows, leaching enhances the dissolution of aquifer minerals, forming new hydrochemical characteristics. Therefore, F1 represents the effect of mineral leaching.

Table 1. Factor analysis for shallow groundwater samples in November (n = 13) [a].

Variable	Components [b]			
	F1	**F2**	**F3**	**F4**
Ca^{2+}	0.94	0.24	−0.06	0.10
NH_4^+	0.91	0.06	−0.28	−0.21
HCO_3^-	0.91	0.37	0.07	0.17
Mg^{2+}	0.88	0.33	−0.10	0.21
EC	0.80	0.51	−0.03	0.30
TDS	0.80	0.51	−0.03	0.30
δ^2H	0.18	0.96	0.02	0.21
Cl^-	0.40	0.91	0.00	0.00
$\delta^{18}O$	0.28	0.85	−0.11	0.36
NA^++K^+	0.55	0.82	−0.02	0.11
Eh	0.00	0.05	0.98	0.13
NO_3^-	−0.05	−0.34	0.91	−0.12
DO	−0.44	0.01	0.87	−0.06
HS^-	−0.46	−0.10	−0.72	−0.30
DOC	0.62	0.40	0.65	0.08
T	−0.31	−0.02	0.64	−0.30
SO_4^{2-}	0.00	0.01	−0.16	0.91
pH	−0.10	−0.33	−0.23	−0.75
Fe^{2+}	0.57	0.45	−0.03	0.67
Mn^{2+}	0.61	0.46	−0.07	0.61
Variance/%	33.75	23.77	20.43	14.65
Cumulative/%	33.75	57.52	77.95	92.61

Notes: [a] Factor loadings (Varimax rotation) [b] Extraction: principal components.

Factor 2 is composed of δ^2H, Cl^-, $\delta^{18}O$, and Na^++K^+ with variance contribution rate of 23.77%, which are positively correlated with F2. There are significant differences in δ^2H, $\delta^{18}O$ values and Na^+, K^+, Cl^- concentrations between river water and regional groundwater. Meanwhile, δ^2H and $\delta^{18}O$ stable isotopes are often used as tracers to analysis groundwater recharge sources. Therefore, F2 indicates the effect of regional groundwater.

The total variances of Eh, DO, NO_3^-, HS^-, DOC, and T in F3 were 20.43%. Eh, DO, and NO_3^- showed strong positive loadings at 0.98, 0.91, and 0.87, respectively. T and DOC showed medium positive loadings (0.65 and 0.64, respectively). Under the condition of sufficient organic carbon in groundwater, aerobic bacteria use O_2 to oxidize organic carbon. When oxygen supply is limited, facultative anaerobic bacteria use NO_3^- and O_2 as electron acceptors. With the decrease of O_2 level, specific anaerobic bacteria begin to use non-oxygen electron acceptors [9]. Denitrifying bacteria are ubiquitous in groundwater and the key limiting factors are the concentration and availability of oxygen and electron

donors [6]. The ΔG° (W) of aerobic respiration and denitrification is similar. It often constitutes the same zoning. Therefore, F3 represents the effect of aerobic respiration and denitrification.

$$CH_2O + O_2 = CO_2 + H_2O \quad (1)$$

$$5CH_2O + 4NO_3^- + 4H^+ \rightarrow 2N_2 + 7H_2O + 5CO_2 \quad (2)$$

F4, which explains 14.65% of the total variance (Table 1), showed strong positive loading for SO_4^{2-}, medium positive loading for Fe^{2+}, Mn^{2+}, and strong negative loading pH. The concentrations of O_2 and NO_3^- in groundwater decreased due to aerobic respiration and denitrification in the process of river water infiltration, which further induced a reducing environment, following which Mn (IV) and Fe (III) reduction and sulfate reduction occurred. The reduction of Mn (IV) and Fe (III) is generally believed to occur successively at low ΔG° (W), and the boundary is distinct. As Eh decreases, sulfate reduction begins to occur in groundwater [49,50].

$$CH_2O + 8H^+ + 4Fe(OH)_3\ (s) \rightarrow 4Fe^{2+} + 11H_2O + CO_2 \quad (3)$$

$$CH_2O + 4H^+ + 4MnO_2\ (s) \rightarrow 2Mn^{2+} + 3H_2O + CO_2 \quad (4)$$

$$2CH_2O + SO_4^{2-} + H^+ \rightarrow HS^- + 2H_2O + 2CO_2 \quad (5)$$

Fe (III) reduction and sulfate reduction often accompany or alternate each other. Fe^{2+} produced by Fe (III) reduction is adsorbed on the mineral surface to inhibit Fe (III) reduction. S^{2-} produced by sulfate reduction can form FeS precipitates with Fe^{2+} and promote the reduction of Fe (III) minerals. Therefore, a certain sulfate reduction rate may be a necessary condition for iron reduction in aquifers. Based on the equilibrium conditions of Fe (III) and sulfate reduction, it is concluded that simultaneous reduction of Fe (III) and sulfate is thermodynamically possible, and sulfate reduction may even occur before Fe (III) reduction [4]. The pH value of pore water also has a strong control on whether iron (III) or sulfate reduction is beneficial. For the same minerals and the same reactant concentration, low pH is more conducive to the reduction of Fe (III) in groundwater and high pH is more conducive to the reduction of SO_4^{2-} in groundwater. Therefore, F4 represents Mn (IV) and Fe (III) reduction and sulfate reduction [6]. According to the variance of each factor, the main factors affecting groundwater chemistry are leaching and regional groundwater mixing, followed by aerobic respiration and denitrification. In contrast, Mn (IV) and Fe (III) reduction and sulfate reduction have the least influence on groundwater chemistry.

3.5. Cluster Analysis

According to the similarity between factor scores, groundwater was divided into four groups through CA, and the results of HCA are presented in Figure 5.

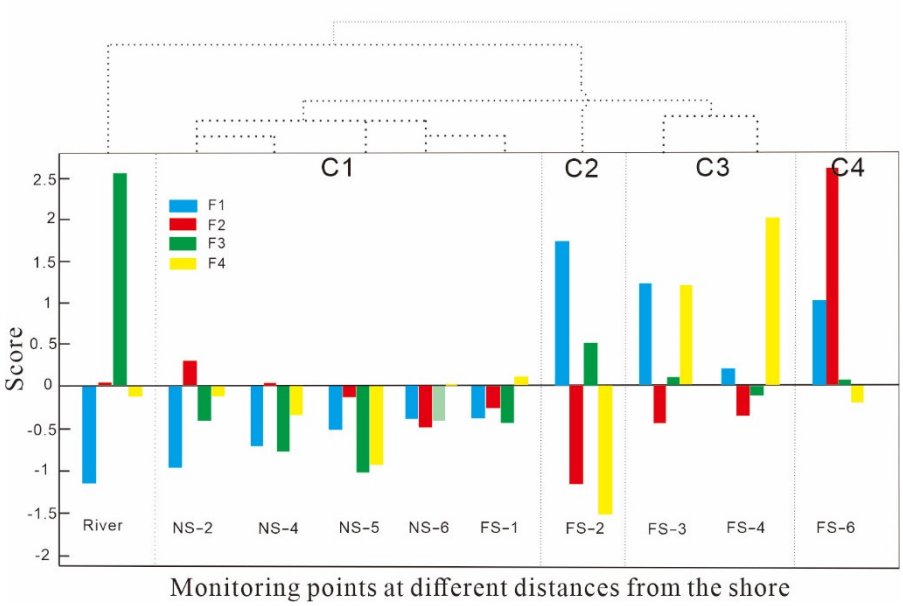

Figure 5. Plots of the variation of factor scores and Hierarchical diagram of groundwater sampling locations.

The first group (C1) includes NS2, NS4, NS5, NS6, and FS1 (within 80 m from shore), which are closer to river water. Figure 6 shows that river water and C1 are mainly controlled by factor F3. F3 has high scores in river water but low scores in observation wells in the C1, indicating that the two can be separated through F3 (aerobic respiration and denitrification). The second group (C2) included FS2 (within 80–200 m from shore) mainly controlled by F1 and F4. The F4 score dropped to the lowest and F1 score was higher. The results indicate that C2 can be distinguished by sulfate reduction and leaching. The third group (C3) including FS3, FS4 (within 200–700m from shore) is mainly controlled by factor F4. The increase of F4 factor score to the highest value indicates that C3 can be distinguished by Mn (IV) and Fe (III) reduction. The fourth group (C4) included FS6 (within 700–1100 m from the shore), mainly controlled by F2. The increase of the score of F2 to the highest value indicates that C4 can be distinguished by regional groundwater mixing. Therefore, according to the geochemical similarity, the flow path can be divided into four different hydrochemical zones.

The $\delta^{18}O$ and $\delta^{2}H$ values in C1 indicate that river water infiltration is the main source of recharge, so C1 is a Strongly Influenced by River Water Zone. The values of $\delta^{18}O$ and $\delta^{2}H$ were −9.42‰ and −74.59‰, respectively, which were slightly higher than those of river water ($\delta^{18}O$ and $\delta^{2}H$ were −9.28‰ and −71.24‰, respectively), indicating that river water infiltration and precipitation were the main recharge sources of C2. The values of $\delta^{18}O$ and $\delta^{2}H$ in C4 decreased to −6.63‰ and −60.77‰, indicating that lateral groundwater recharge in the region increased significantly. The values of $\delta^{18}O$ and $\delta^{2}H$ in C4 decreased to −6.63‰ and −60.77‰, indicating that lateral groundwater recharge in the region increased significantly.

In summary, groundwater could be divided into four main geochemical zones by CA: (1) C1: the Zone Strongly Influenced by River Water; (2) C2: the Zone Moderately Influenced by River Water; (3) C3: the Zone Weakly Influenced by River Water; and (4) C4: the Zone Strongly Influenced by Regional Groundwater. This is similar to the results obtained by Su, et al. using the traditional hydrogeochemical analysis method [16].

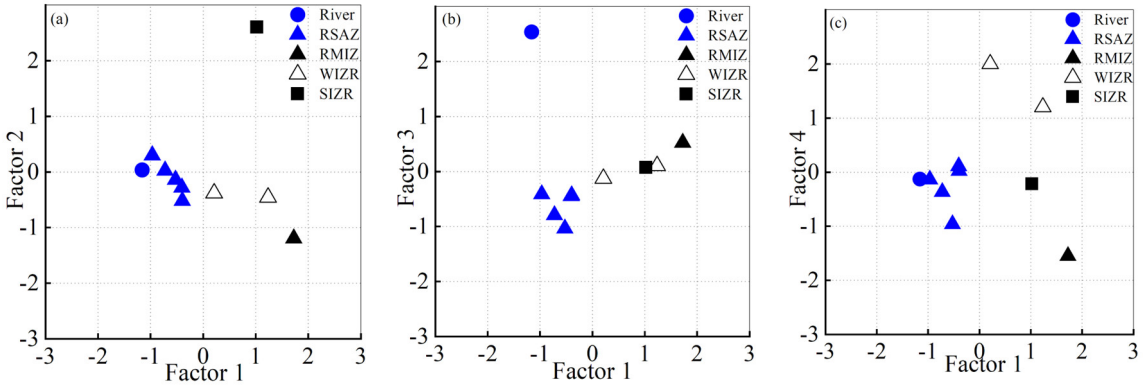

Figure 6. Plots of four factor scores showing the distribution of HCA-derived clusters: (**a**) factor 1 vs. factor 2; (**b**) factor 1 vs. factor 2; and (**c**) factor 1 vs. factor 3.

4. Hydrogeochemical of Each Geochemical Zones

4.1. The Zone Strongly Influenced by River Water (C1)

River water infiltration transports a large amount of DO into groundwater. As oxygen and organic carbon oxidation can provide the most energy for microorganisms, microorganisms tend to preferentially consume O_2 to oxidize organic carbon [9]. When sufficient organic carbon is available, aerobic bacteria will continue to use DO until it is depleted, which explains the rapid decrease of DO concentration from 8.32 to 0.48 mg/L when river water infiltration reached NS2. After the depletion of DO, facultative anaerobic bacteria (aerobic or anaerobic bacteria) use NO_3^- as an electron acceptor, in which explains the rapid reduction of NO_3^--N from 2.28 to 0.73 mg/L when river water infiltrated NS2. F3 representing aerobic respiration and denitrification exhibited high scores in river water and low scores in C1 (Figure 7), indicating the occurrence of strong aerobic respiration and denitrification during the infiltration of river water in C1, and O_2 and NO_3^- from were depleted in river water, resulting in extremely low DO and NO_3^- concentrations in C1 groundwater.

The variation of Mn^{2+} from NS1 to NS2 was the largest, increasing from 0.20 mg/L to 0.96 mg/L, and the variation of Fe^{2+} from NS5 to NS6 was the largest, increasing from 0.05 mg/L to 3.81 mg/L. SO_4^{2-} decreased from 37.86 mg/L to 26.23 mg/L from NS4 to NS6. In addition, the fluctuation of F4 scores in the coastal zone (Figure 7) indicates that Mn (IV), Fe (III), and SO_4^{2-} reduction occurred in this zone. But the scores of F1 and F4 were negative for the river and C1 and showed little change. Groundwater in this area is mainly affected by aerobic respiration and denitrification, while Mn (IV), Fe (III), and SO_4^{2-} reduction and leaching have little effect on groundwater chemistry.

In summary, strong aerobic respiration and denitrification occurred within 2 m from the bank when river water infiltrated the strong influence zone of river water. NS2–NS3 (2–5 m from the bank) was the main Mn (IV) reduction zone, and NS5–NS6 (15–30 m from the bank) was the main Fe (III) reduction zone. Sulfate reduction was relatively weak along NS4–NS6 (8–30 m from the bank), which also showed that under the dual impact of pH and Eh, sulfate reduction can accompany or even occur ahead of Fe (III) reduction. The reduction of Mn (IV), Fe (III), and SO_4^{2-} was relatively weak in C1, which may be because the low DOC concentration affects the activity of microorganisms. The average DOC concentration in C1 was 8.98 mg/L, while that in C2, C3, and C4 was 23.32 mg/L).

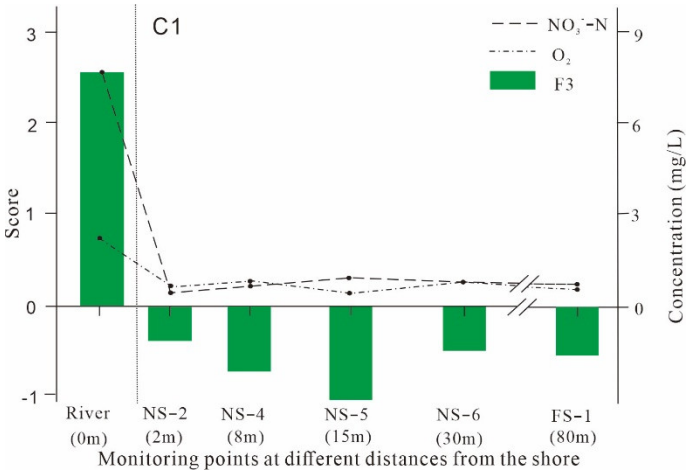

Figure 7. Factor scores and component concentrations in C1.

4.2. The Zone Moderately Influenced by River Water (C2)

With the decrease of groundwater hydraulic gradient (from 8.62‰ to 2.12‰), the flow velocity decreased, the recharge ratio of river water decreased, and the recharge ratio of regional groundwater and precipitation increased. The decrease of flow velocity leads to the increase of the influence of leaching on hydrogeochemistry and the increase of Ca^{2+}, Mg^{2+} and HCO_3^- concentrations. Strong sulfate reduction accompanied by Fe^{2+} precipitation occurred. Moreover, SO_4^{2-} concentration decreased from 30.42 to 11.18 mg/L and Fe^{2+} concentration decreased from 1.74 mg/L to 0.28 mg/L.

The score of F4 decreased to the lowest and that of F1 increased significantly, indicating that C2 was mainly controlled by sulfate reduction and mineral leaching (Figure 8).

It is worth noting that Eh in the medium influence zone of river water was −63.00 mV, which is higher than that in C1 (average of −164 mV), but the intensity of sulfate reduction was significantly higher than that of Fe (III) reduction and sulfate reduction in C1. The average pH value in C2 was 8.83, which is significantly higher than the average pH value in NS6–FS1 (average of 7.67). This is due to the presence of $CaCO_3$ in sediments and its buffering effect on pore water pH, gradually increasing pH. As the reduction of Mn (IV), Fe (III), and SO_4^{2-} is not only affected by redox conditions, but also by mineral species and groundwater pH, and there was no significant change in the mineral composition of the aquifer along the flow path, the change from Fe (III) reduction to sulfate reduction in groundwater is more likely to be explained by the increase of pH, which favors sulfate reduction over Fe (III) reduction [6,51].

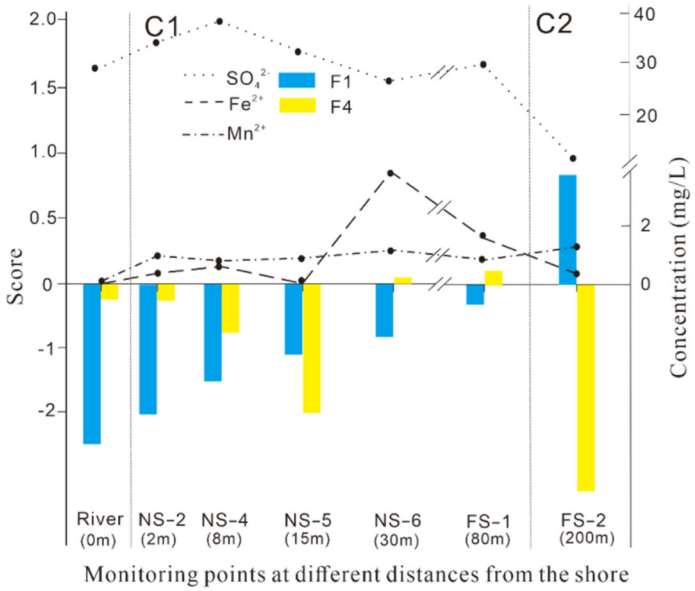

Figure 8. Factor scores and component concentrations in C1 and C2.

4.3. The Zone Weakly Influenced by River Water (C3)

The average concentrations of Fe^{2+} and Mn^{2+} in the band were 12.78 mg/L and 5.39 mg/L, respectively, which were significantly higher than those in C1 and C2. The concentration of SO_4^{2-} was 64.62 mg/L, which was significantly higher than that of C1 and C2. Reoxygenation of groundwater changes the redox conditions from sulfate reduction to Mn (IV), Fe (III) reduction [35,36]. There are three main reasons for the reoxidation of the groundwater in the process of river water infiltration. (1) Oxygen-containing rainwater enters the groundwater through the permeable unsaturated zone. (2) Oxygen directly diffuses into the groundwater through the unsaturated zone. (3) Groundwater level oscillation and bubble inclusion. Among them, groundwater level oscillation and air inclusion are the main reasons for groundwater reoxidation. The groundwater is still dominated by Fe (III) mineral reduction, and the concentration of Fe^{2+} increases.

NO_3^- and O_2 supplied vertically in reductive groundwater are consumed rapidly. Consequently, a low amount of Fe^{2+} is directly oxidized and precipitated by O_2 in groundwater. The groundwater is still dominated by Fe (III) mineral reduction, and the concentration of Fe^{2+} increases. SO_4^{2-} concentration has little effect on the equilibrium between SO_4^{2-} and Fe (III) reduction. This equilibrium is mainly controlled by groundwater redox conditions, groundwater pH, and mineral species. As the mineral species of the aquifer along the flow path did not change significantly, pH was the main factor affecting the balance between sulfate reduction and Fe (III) reduction. The dissolved CO_2 produced by microbial consumption of organic carbon in groundwater reduces the pH value of groundwater, resulting in the decrease of pH to 7.31 in C2, which is significantly lower than that of C2 (pH 8.83). In the Fe^{2+} rich environment, the pH value of pore water strongly controls the occurrence of Fe (III) or sulfate reduction, which also leads to the terminal electron-accepting process (TEAP) from sulfate to Fe (III) [6,51]. The score of F4 increased to the highest value, indicating strong Mn (IV) and Fe (III) reduction (Figure 9).

The groundwater hydraulic gradient of FS4 is 2.63‰, higher than that of FS3 (2.12‰). The greater the flow rate of groundwater, the shorter the contact time between groundwater and aquifer minerals, and the weaker the effect of leaching on groundwater chemistry, resulting in lower concentrations of Ca^{2+}, Mg^{2+}, HCO_3^- and other components in groundwater. In C3, the score of F1 significantly varies between FS3 and FS4, which also indicates a difference in the effect of leaching on groundwater chemistry(Figure 9).

In the zone, and the changes of Na^+, Cl^-, NO_3^-, and DO concentrations were relatively small. The low scores of F2 and F3 in the weak influence zone of river water indicated that

the mixing effect, aerobic respiration, and denitrification had weak effects on groundwater chemistry.

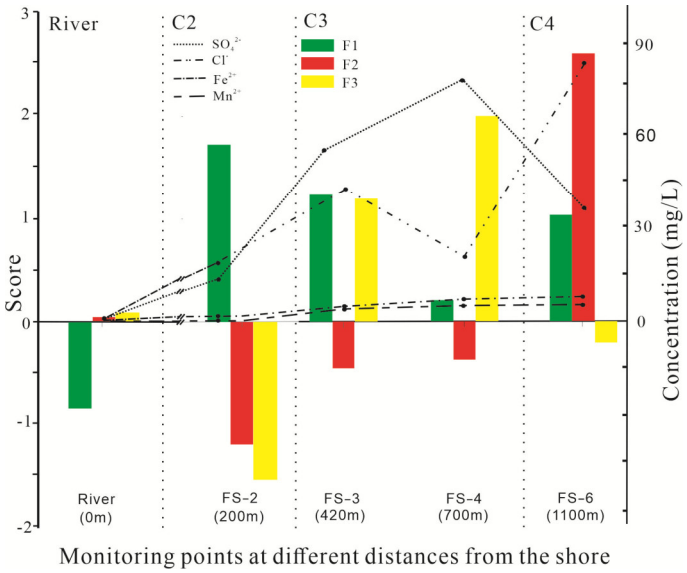

Figure 9. Factor scores and component concentrations in C2, C3 and, C4.

4.4. The Zone Strongly Influenced by Regional Groundwater (C4)

The concentrations of Na^+, K^+, and Cl^- were high in the regional groundwater. Further, their concentrations increased along FS5–FS6 in C4 due to the mixing effect of regional groundwater. The high score of F2 indicates that the mixing effect of regional groundwater is the main influencing factor of groundwater chemistry in C4 (Figure 9).

The concentrations of Fe^{2+} and SO_4^{2-} in FS5 were 0.04 mg/L and 26.87 mg/L, respectively, which are significantly lower than those in the weak influence zone of river water. This suggests that strong SO_4^{2-} reduction occurred in the strong influence zone of regional groundwater, accompanied by the precipitation of Fe^{2+}.

The Eh value at FS5 (850 m away from the bank) in the strong influence zone of regional groundwater was −145, which is significantly lower than that in the weak influence zone of river water (−65.5). The enhancement of reducing groundwater conditions is more conducive to SO_4^{2-} reduction. At the same time, the pH value of FS5 was 9.62, which is significantly higher than that of the weak influence zone of river water (7.31). High pH is also conducive to SO_4^{2-} reduction. Furthermore, HS^- from SO_4^{2-} reduction precipitates with Fe^{2+}, decreasing the concentration of Fe^{2+} in groundwater. The scores of F4 in the C4 were low, significantly differing from those in C3 also suggests that sulfate red

uction occurred in this place.

The concentrations of Ca^{2+}, Mg^{2+}, HCO_3^- and other components in groundwater in C4 increased. This is because C4 is located far away from the center of the funnel, the hydraulic gradient is reduced, the flow rate is slowed down, the contact time between groundwater and aquifer minerals is prolonged, and the leaching effect on groundwater chemistry is strengthened. The increase in F1 indicates the enhancement of dissolution and filtration in the strong influence zone of regional groundwater (Figure 9).

5. Conclusions

The MSA method was used to analyze hydrogeochemical interactions between river water and groundwater during river water infiltration. Through FA, the following main factors controlling groundwater quality were extracted: (1) leaching (2) regional groundwater influence (3) aerobic respiration and denitrification (4) Mn (IV) and Fe (III) reduction and sulfate reduction. Through HCA, the study area was divided into four different

hydrogeochemical influence areas (C1–C4), and the main influencing factors in each region were identified by factor scores. The main influencing factors of groundwater chemical change were comprehensively analyzed by combining the results of MSA analysis with hydrochemical indexes, hydrodynamic conditions, and recharge and discharge conditions.

The results show that the zone strongly influenced by river water (C1) is mainly controlled by aerobic respiration and denitrification, the zone moderately influenced by river water (C2) is mainly controlled by sulfate reduction, the zone weakly influenced by river water (C3) is mainly controlled by Mn (IV) and Fe (III) mineral reduction, and the zone strongly influenced by regional groundwater (C4) is mainly controlled by regional groundwater mixing. The leaching effect is mainly affected by the hydraulic gradient of groundwater.

This study evaluated the hydrogeochemical effect and determined the key factors controlling groundwater quality during Bank filtration. The research results are expected to help managers establish a better groundwater management model for riverside well field. In the future research, multivariate statistical analysis will be used to analyze the influence of seasonal variation on hydrogeochemistry in the process of reservoir bank filtration.

Author Contributions: Conceptualization, Y.C. and Y.B.; methodology, Y.B.; software, Y.B.; formal analysis, Y.B. and Y.C.; data curation, Q.C.; writing—original draft preparation, Y.B., Y.C., Q.C.,Y.S. and Y.Z.; writing—review and editing, Y.B., Y.C., Q.C.; visualization, Y.B.; supervision, Y.C. All authors have read and agreed to the published version of the manuscript.

Funding: This work was supported by the National Natural Science Foundation of China ,Grant numbers: 41877178, 41372238 and the Geological Exploration Fund of Qinghai Provincial Bureau of Geological and Mineral Exploration and Development : Qingdi Mining Section (2020) No. 25.

Data Availability Statement: Not applicable.

Acknowledgments: The authors would like to thank the editors and reviewers of Water for their thoughtful and constructive comments, which helped improve this paper substantially.

Conflicts of Interest: The authors declare no conflict of interest.

References

1. Kareem, S.L.; Mohammed, A.A. Removal of Tetracycline from Wastewater Using Circulating Fluidized Bed. *Iraqi J. Chem. Pet. Eng.* **2020**, *21*, 29–37. https://doi.org/10.31699/ijcpe.2020.3.4.
2. Kareem, S.L.; Jaber, W.S.; Al-Maliki, L.A.; Al-Husseiny, R.A.; Al-Mamoori, S.K.; Alansari, N. Water quality assessment and phosphorus effect using water quality indices: Euphrates River- Iraq as a case study. *Groundw. Sustain. Dev.* **2021**, *14*, 100630. https://doi.org/10.1016/j.gsd.2021.100630.
3. Greskowiak, J.; Prommer, H.; Massmann, G.; Nützmann, G. Modeling Seasonal Redox Dynamics and the Corresponding Fate of the Pharmaceutical Residue Phenazone During Artificial Recharge of Groundwater. *Environ. Sci. Technol.* **2006**, *40*, 6615–6621. https://doi.org/10.1021/es052506t.
4. Hamann, E.; Stuyfzand, P.J.; Greskowiak, J.; Timmer, H.; Massmann, G. The fate of organic micropollutants during long-term/long-distance river bank filtration. *Sci. Total Environ.* **2016**, *545–546*, 629–640. https://doi.org/10.1016/j.scitotenv.2015.12.057.
5. Munz, M.; Oswald, S.E.; Schäfferling, R.; Lensing, H.-J. Temperature-dependent redox zonation, nitrate removal and attenuation of organic micropollutants during bank filtration. *Water Res.* **2019**, *162*, 225–235. https://doi.org/10.1016/j.watres.2019.06.041.
6. Postma, D.; Jakobsen, R. Redox zonation: Equilibrium constraints on the Fe (III)/SO_4-reduction interface. *Geochim. Cosmochim. Acta* **1996**, *60*, 3169–3175.
7. Massmann, G.; Pekdeger, A.; Merz, C. Redox processes in the Oderbruch polder groundwater flow system in Germany. *Appl. Geochem.* **2004**, *19*, 863–886.
8. Rivett, M.O.; Buss, S.R.; Morgan, P.; Smith, J.W.N.; Bemment, C.D. Nitrate attenuation in groundwater: A review of biogeochemical controlling processes. *Water Res.* **2008**, *42*, 4215–4232. https://doi.org/10.1016/j.watres.2008.07.020.
9. Korom, S.F. Natural denitrification in the saturated zone: A review. *Water Resour. Res.* **1992**, *28*, 1657–1668.
10. Jung, H.B.; Zheng, Y.; Rahman, M.W.; Rahman, M.M.; Ahmed, K.M. Redox zonation and oscillation in the hyporheic zone of the Ganges-Brahm-Meghna Delta: Implications for the fate of groundwater arsenic during discharge. *Appl. Geochem.* **2015**, *63*, 647–660.

11. Gandy, C.; Smith, J.; Jarvis, A. Attenuation of mining-derived pollutants in the hyporheic zone: A review. *Sci. Total Environ.* **2007**, *373*, 435–446. https://doi.org/10.1016/j.scitotenv.2006.11.004.
12. Su, X.; Lu, S.; Gao, R.; Su, D.; Yuan, W.; Dai, Z.; Papavasilopoulos, E.N. Groundwater flow path determination during riverbank fifiltration affected by groundwater exploitation: A case study of Liao River, Northeast China. *Hydrol. Sci. J.* **2017**, *62*, 2331–2347.
13. Kedziorek, M.A.M.; Geoffriau, S.; Bourg, A.C.M. Organic Matter and Modeling Redox Reactions during River Bank Filtration in an Alluvial Aquifer of the Lot River, France. *Environ. Sci. Technol.* **2008**, *42*, 2793–2798. https://doi.org/10.1021/es702411t.
14. Hancock, P.J. Human Impacts on the Stream-Groundwater Exchange Zone. *Environ. Manag.* **2002**, *29*, 763–781. https://doi.org/10.1007/s00267-001-0064-5.
15. Gibert, J.; Fournier, F.; Mathieu, J. *Ground Water/Surface Water Ecotone*; Cambridge University Press: New York, NY, USA, 1997.
16. Su, X.; Chen, Y.; Lyu, H.; Shi, Y.; Wan, Y.; Zhang, Y. Response of redox zonation to recharge in a riverbank filtration system: A case study of the Second Songhua river, NE China. *Water Policy* **2020**, *51*, 1104–1119. https://doi.org/10.2166/nh.2020.108.
17. Burt, T.P.; Pinay, G.; Matheson, F.E.; Haycock, N.E.; Buttruini, A.; Clement, J.C.; Danielescu, S.; Dowrick, D.J.; Hefting, M.M.; Hillbrichtllkowaka, A.; Maitre, V. Water table flfluctuations in the riparian zone: Comparative results from a pan-European experiment. *J. Hydrol.* **2002**, *265*, 129–148.
18. Massmann, G.; Nogeitzig, A.; Taute, T.; Pekdeger, A. Seasonal and spatial distribution of redox zones during lake bank filtration in Berlin, Germany. *Environ. Earth Sci.* **2007**, *54*, 53–65. https://doi.org/10.1007/s00254-007-0792-9.
19. Kohfahl, C.; Massmann, G.; Pekdeger, A. Sources of oxygen flux in groundwater during induced bank filtration at a site in Berlin, Germany. *Appl. Hydrogeol.* **2009**, *17*, 571–578. https://doi.org/10.1007/s10040-008-0389-8.
20. Wang, P.; Yao, J.; Wang, G.; Hao, F.; Shrestha, S.; Xue, B.; Xie, G.; Peng, Y. Exploring the application of artificial intelligence technology for identification of water pollution characteristics and tracing the source of water quality pollutants. *Sci. Total Environ.* **2019**, *693*, 133440. https://doi.org/10.1016/j.scitotenv.2019.07.246.
21. Zhao, J.; Fu, G.; Lei, K.; Li, Y. Multivariate analysis of surface water quality in the Three Gorges area of China and implications for water management. *J. Environ. Sci.* **2011**, *23*, 1460–1471. https://doi.org/10.1016/s1001-0742(10)60599-2.
22. Liu, P.; Hoth, N.; Drebenstedt, C.; Sun, Y.; Xu, Z. Hydro-geochemical paths of multi-layer groundwater system in coal mining regions—Using multivariate statistics and geochemical modeling approaches. *Sci. Total Environ.* **2017**, *601–602*, 1–14. https://doi.org/10.1016/j.scitotenv.2017.05.146.
23. Ta, M.; Zhou, X.; Guo, J.; Wang, X.; Wang, Y.; Xu, Y. The Evolution and Sources of Major Ions in Hot Springs in the Triassic Carbonates of Chongqing, China. *Water* **2020**, *12*, 1194. https://doi.org/10.3390/w12041194.
24. Sharma, G.; Lata, R.; Thakur, N.; Bajala, V.; Kuniyal, J.C.; Kumar, K. Application of multivariate statistical analysis and water quality index for quality characterization of Parbati River, Northwestern Himalaya, India. *Discov. Water* **2021**, *1*, 5. https://doi.org/10.1007/s43832-021-00005-3.
25. Gad, M.; Saleh, A.H.; Hussein, H.; Farouk, M.; Elsayed, S. Appraisal of Surface Water Quality of Nile River Using Water Quality Indices, Spectral Signature and Multivariate Modeling. *Water* **2022**, *14*, 1131.
26. Gad, M.; Osta, M.E.; Geochemical controlling mechanisms and quality of the groundwater resources in El Fayoum Depression, Egypt. *Arab. J. Geosci.* **2020**, *13*, 861.
27. Suk, H.; Lee, K.-K. Characterization of a Ground Water Hydrochemical System Through Multivariate Analysis: Clustering into Ground Water Zones. *Groundwater* **1999**, *37*, 358–366. https://doi.org/10.1111/j.1745-6584.1999.tb01112.x.
28. Choi, B.-Y.; Kim, H.-J.; Kim, K.; Kim, S.-H.; Jeong, H.-J.; Park, E.; Yun, S.-T. Evaluation of the processes affecting vertical water chemistry in an alluvial aquifer of Mankyeong Watershed, Korea, using multivariate statistical analyses. *Environ. Earth Sci.* **2007**, *54*, 335–345. https://doi.org/10.1007/s00254-007-0820-9.
29. Zuo, R.; Xue, Z.; Wang, J.; Meng, L.; Zhao, X.; Pan, M.; Cai, W. Spatiotemporal variations of redox conditions and microbial responses in a typical river bank filtration system with high Fe2+ and Mn2+ contents. *J. Hydrol.* **2022**, *609*, 127777. https://doi.org/10.1016/j.jhydrol.2022.127777.
30. Su, X.; Zheng, Z.; Chen, Y.; Wan, Y.; Lyu, H.; Dong, W. Effects of carbon load on nitrate reduction during riverbank filtration: Field monitoring and batch experiment. *Sci. Total. Environ.* **2022**, *845*, 157198. https://doi.org/10.1016/j.scitotenv.2022.157198.
31. Chen, Y.; Su, X.; Wan, Y.; Lyu, H.; Dong, W.; Shi, Y.; Zhang, Y. Nitrogen biogeochemical reactions during bank filtration constrained by hydrogeochemical and isotopic evidence: A case study in a riverbank filtration site along the Second Songhua River, NE China. *Appl. Geochem.* **2022**, *140*, 105272. https://doi.org/10.1016/j.apgeochem.2022.105272.
32. Ren, W.; Su, X.; Zhang, X.; Chen, Y.; Shi, Y. Influence of hydraulic gradient and temperature on the migration of E. coli in saturated porous media during bank filtration: A case study at the Second Songhua River, Songyuan, Northeastern China. *Environ. Geochem. Health* **2020**, *42*, 1977–1990. https://doi.org/10.1007/s10653-019-00459-4.
33. Papaioannou, A.; Mavridou, A.; Hadjichristodoulou, C.; Papastergiou, P.; Pappa, O.; Dovriki, E.; Rigas, I. Application of multivariate statistical methods for groundwater physicochemical and biological quality assessment in the context of public health. *Environ. Monit. Assess.* **2010**, *170*, 87–97. https://doi.org/10.1007/s10661-009-1217-x.
34. Adhikari, K.; Mal, U. Application of multivariate statistics in the analysis of groundwater geochemistry in and around the open cast coal mines of Barjora block, Bankura district, West Bengal, India. *Environ. Earth Sci.* **2019**, *78*, 72. https://doi.org/10.1007/s12665-019-8071-0.
35. Davis, J.C.; Statistics and data analysis in geology. Wiley, New York 1973.
36. Sikdar, P.K.; Chakraborty, S. Genesis of arsenic in groundwater of North Bengal Plain using PCA: A case study of English Bazar Block, Malda District, West Bengal, India. *Hydrol. Process.* **2009**, *22*, 1796–1809. https://doi.org/10.1002/hyp.6742.

37. Kaiser, H.F. The Application of Electronic Computers to Factor Analysis. *Educ. Psychol. Meas.* **1960**, *20*, 141–151. https://doi.org/10.1177/001316446002000116.
38. Vega, M.; Pardo, R.; Barrado, E.; Debán, L. Assessment of seasonal and polluting effects on the quality of river water by exploratory data analysis. *Water Res.* **1998**, *32*, 3581–3592. https://doi.org/10.1016/s0043-1354(98)00138-9.
39. Wayland, K.G.; Long, D.T.; Hyndman, D.W.; Pijanowski, B.C.; Woodhams, S.M.; Haack, S.K. Identifying relationships between baseflow geochemistry and land use with synoptic sampling and r-mode factor analysis. *J. Environ. Qual.* **2003**, *32*, 180–190.
40. Steinhorst, R.K.; Williams, R.E. Discrimination of Groundwater Sources Using Cluster Analysis, MANOVA, Canonical Analysis and Discriminant Analysis. *Water Resour. Res.* **1985**, *21*, 1149–1156. https://doi.org/10.1029/wr021i008p01149.
41. Güler, C.; Thyne, G.D.; McCray, J.E.; Turner, A.K. Evaluation of graphical and multivariate statistical methods for classification of water chemistry data. *Hydrogeol. J.* **2002**, *10*, 455–474. https://doi.org/10.1007/s10040-002-0196-6.
42. Davis, J.C. Statistics and data analysis in geology, 2nd edn. Wiley, New York, 1986, p. 646.
43. Adar, E.; Rosenthal, E.; Issar, A.; Batelaan, O. Quantitative assessment of the flow pattern in the southern Arava Valley (Israel) by environmental tracers and a mixing cell model. *J. Hydrol.* **1992**, *136*, 333–352. https://doi.org/10.1016/0022-1694(92)90017-p.
44. Schot, P.; van der Wal, J. Human impact on regional groundwater composition through intervention in natural flow patterns and changes in land use. *J. Hydrol.* **1992**, *134*, 297–313. https://doi.org/10.1016/0022-1694(92)90040-3.
45. Spanos, T.; Ene, A.; Xatzixristou, C. Assessmeny of groundwater quality and hydrogeological profile of kavala area, Northern Greece. *Rom. J. Phys.* **2015**, *60*, 1139–1150.
46. Liu, C.-W.; Lin, K.-H.; Kuo, Y.-M. Application of factor analysis in the assessment of groundwater quality in a blackfoot disease area in Taiwan. *Sci. Total Environ.* **2003**, *313*, 77–89. https://doi.org/10.1016/s0048-9697(02)00683-6.
47. Guo, X.; Zuo, R.; Wang, J.; Meng, L.; Teng, Y.; Shi, R.; Gao, X.; Ding, F. Hydrogeochemical Evolution of Interaction Between Surface Water and Groundwater Affected by Exploitation. *Groundwater* **2019**, *57*, 430–442. https://doi.org/10.1111/gwat.12805.
48. Dash, R.R.; Bhanu Prakash, E.V.P.; Kumar, P.; Mehrotra, I.; Sandhu, C.; Grischek, T. River bank filtration in Haridwar, India: Removal of turbidity, organics and bacteria. *Hydrogeol. J.* **2010**, *18*, 973–983. https://doi.org/10.1007/s10040-010-0574-4.
49. Champ, D.R.; Gulens, J.; Jackson, R.E. Oxidation–reduction sequences in ground water flow systems. *Can. J. Earth Sci.* **1979**, *16*, 12–23. https://doi.org/10.1139/e79-002.
50. Kedziorek, M.A.; Bourg, A.C. Electron trapping capacity of dissolved oxygen and nitrate to evaluate Mn and Fe reductive dissolution in alluvial aquifers during riverbank filtration. *J. Hydrol.* **2009**, *365*, 74–78. https://doi.org/10.1016/j.jhydrol.2008.11.020.
51. Gad, M.; Dahab, K.; Ibrahim, H. Impact of iron concentration as a result of groundwater exploitation on the Nubian sandstone aquifer in El Kharga Oasis, western desert, Egypt. *NRIAG J. Astron. Geophys.* **2016**, *5*, 216–237. https://doi.org/10.1016/j.nrjag.2016.04.003.